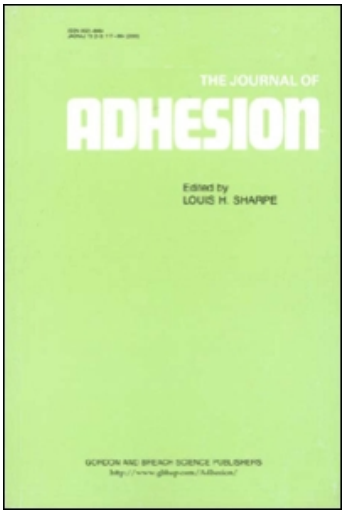

The Journal of Adhesion
Publication details, including instructions for authors and subscription information:
http://www.informaworld.com/smpp/title~content=t713453635

Nanoscale characterisation of thickness and properties of interphase in polymer matrix composites

Jang-Kyo Kim[a]; Alma Hodzic[b]
[a] Department of Mechanical Engineering, Hong Kong University of Science and Technology, Kowloon, Hong Kong [b] Cooperative Research Centre for Polymers, Department of Applied Chemistry, Royal Melbourne Institute of Technology, Melbourne, Australia

Online publication date: 08 September 2010

To cite this Article Kim, Jang-Kyo and Hodzic, Alma(2003) 'Nanoscale characterisation of thickness and properties of interphase in polymer matrix composites', The Journal of Adhesion, 79: 4, 383 — 414
To link to this Article: DOI: 10.1080/00218460309585
URL: http://dx.doi.org/10.1080/00218460309585

The Journal of Adhesion, 79: 383–414, 2003

0021-8464/03 $12.00 +.00
DOI: 10.1080/00218460390148185

Taylor & Francis
Taylor & Francis Group

NANOSCALE CHARACTERISATION OF THICKNESS AND PROPERTIES OF INTERPHASE IN POLYMER MATRIX COMPOSITES

Jang-Kyo Kim
Department of Mechanical Engineering,
Hong Kong University of Science and Technology,
Clear Water Bay, Kowloon, Hong Kong

Alma Hodzic
Cooperative Research Centre for Polymers,
Department of Applied Chemistry,
Royal Melbourne Institute of Technology,
Melbourne, Australia

An overview is presented of the properties and effective thickness of the interphase formed between fibres and polymer matrices. Chemical and physical characterization of the interphase is discussed to portray molecular interactions comprising the interphase layers in silane-treated glass-fibre composites. The gap between physico-chemical investigation on one side and bulk material testing on the other side is bridged by implementation of novel techniques, such as nanoindentation, nanoscratch tests, and atomic force microscopy (AFM), which have been successfully used for nanoscopic characterization of the interphase in the past few years.

Received 18 September 2001; in final form 10 July 2002.

This article is one of a collection of articles honoring Hatsuo (Ken) Ishida, the recipient in February 2001 of *The Adhesion Society Award for Excellence in Adhesion Science, Sponsored by 3M*.

The author wishes to thank past and present colleagues—S. L. Gao, M. L. Sham, Z. H. Stachurski, and J. S. Wu—for their contributions to this work. They are also grateful to E. Mäder of the Institute of Polymer Research, Germany, as well as to J. J. Kellar of South Dakota School of Mines and Technology, USA, for kindly providing unpublished/published manuscripts with original illustrations that form part of this paper. The financial support by the Hong Kong Research Grant Council (RGC) is also acknowledged. The mechanical tests and the microscopy were conducted with the technical support of the Advanced Engineering Materials Facilities (AEMF) and Materials Characterisation and Preparation Facilities (MCPF) at Hong Kong University of Science and Technology (HKUST).

Address correspondence to Jang-Kyo Kim, Department of Mechanical Engineering, Hong Kong University of Science and Technology, Clear Water Bay, Kowloon, Hong Kong. E-mail: mejkkim@ust.hk

Salient differences are identified between the major findings of these studies in terms of hardness/modulus of the interphase relative to the bulk matrix material. While there is a significant "fibre stiffening" effect that may cause misinterpretation of the interphase hardness very close to the fibre, the formation of both a softer and a harder interphase is possible, depending on the combination of reinforcement, matrix, and coupling agent applied. This is explained by different interdiffusion behaviour, chemical reactions, and molecular conformation taking place at the interphase region in different composite systems. The effective interphase thickness is found to vary from as small as a few hundred nanometers to as large as 10 μm, depending on the constituents, coupling agent, and ageing conditions.

Keywords: Interphase thickness; Nanoscale characterization; Nanoindentation; Nanoscratch test; Atomic force microscopy; Polymer matrix composites; Silane coupling agent; Glass fibre

INTRODUCTION

A bond is formed in fibre-reinforced polymer matrix composites by chemical and physical processes, including interdiffusion of atoms or molecules, cross-linking, immobilization, and crystallization of thermoplastic. The "interphase" generated thereby is a region with finite volume extending from the physical boundaries shared with the fibre and matrix. The interphase may possess chemical, physical, microstructural, and mechanical properties that differ from those of the bulk fibre and matrix, depending on the physico-chemical processes and the type of fibre and matrix materials involved [1, 2]. The existence of the interphase has been substantiated using various techniques, notably by Ishida and coworkers based on Fourier transform infrared (FTIR) spectroscopy [3–7]. The properties of an interphase are governed mainly by the chemical, morphological nature, and thermodynamic compatibility between the fibre and the surrounding matrix. Each fibre-matrix interphase is unique as are the component properties, molecular conformation, environmental conditions, and the manufacturing processes. The interphase usually represents the weakest region in a composite and often limits the overall performance of the bulk material. There is a substantial amount of evidence available regarding the effect of interphase properties on strength, stiffness, and fracture resistance in various failure modes and loading configurations [8, 9]. Many studies confirm that the mechanical/functional performance and the structural integrity of composites could be tailored by altering the properties of the interphase.

Glass fibres, with which the present study is mainly concerned, have been extensively used for over four decades now, accounting for 95% of fibre reinforcement in the current composite industry, partly

due to the development of silane coupling agents. During the manufacturing processes, glass fibres are coated with a size containing lubricants, emulsified polymers, and coupling agents dissolved in an aqueous mixture [10]. The relative amounts of the various components for a typical glass fibre size for thermosetting resins are as follows: antistats 3%, lubricant 4%, surfactant 4%, silane agent 10%, and film former 79% of the total glass fibre surface layer [11]. The film former is a suspension of low molecular weight polymer particles (typically polyvinyl acetate and epoxy) in an aqueous medium. These sizing components adsorb at the fibre surface upon complete drying of the solutions. They remain in high concentration at the fibre-matrix interface and may be dissolved into the matrix during curing of the matrix resin. As there are many processing parameters that influence the performance of the final product, the optimization of sizing constituents, thickness, and processing conditions is essential to the final reinforcement quality. When the glass fibres are treated with a sizing solution containing silane, three layers with different chemical structures and physical properties are formed [12, 13]: (1) physisorbed region, the outermost layer that consists mainly of bulk of the deposited silane; (2) chemisorbed region, the next layer that possesses better resistance to hydrolysis than the physisorbed region; and (3) chemically reacted region, the innermost region next to the glass surface that consists of a three-dimensional network of siloxane, which is very stable and resistant to extraction even by hot water. The physisorbed region comprises the major fraction (as much as 98% of the total deposited silane) consisting of the hydrolyzate of silane physically adsorbed to the glass surface. The thickness and orientation of each region depend on many factors, including deposition conditions, topography of the glass surface, and the concentration of each sizing component in the solution.

The silane coupling agents provide a physico-chemical link between the glass surface and the polymer matrix [14, 15]. Amongst various theories proposed to explain the interfacial bonding mechanisms of silane coupling agent that are responsible for the improvement of the mechanical performance of composites, the most widely accepted is chemical bonding [5, 16]. In the chemical bonding theory, the bifunctional silane molecules act as a link between the glass fibre and resin by forming a chemical bond with the glass surface through a siloxane bridge, whereas its organofunctional group bonds to the polymeric resin. The coreactivity with glass and polymer *via* covalent primary bonds provides molecular continuity across the interface region [17]. The multifunctional organosilanes of formula $X_3Si\text{-}R$ also protect the fibres from adverse hydrolysis effects, one of the major

problems in early composites [4, 5]. Here, the R- group includes vinyl, γ-aminopropyl, and γ-methacryloxypropyl that can react with the polymeric resin, whereas X is such a group as chloro, methoxy, or ethoxy that can hydrolyze to form a silanol group in aqueous solution and thereby react with a hydroxyl group of the glass surface. In addition to the above chemical bonding theory, also widely accepted is the formation of an interpenetrating network (IPN) through interdiffusion [5, 15]. Figure 1a presents a schematic model for interdiffusion and creation of an IPN in a silane-treated glass-fibre composite [18]. Interdiffusion and intermixing take place in the coupling agent-polymer resin interface region, due to penetration of resin into the chemisorbed silane layer and migration of the physisorbed silane molecules into the resin phase. The migration and intermixing of silane and other sizing ingredients with polymer resin inevitably create an interphase of substantial thickness. The large differences in composition and chemical characteristics of the individual sizing components, such as antistats, lubricant, surfactant, and film former, further complicate the formation of the interphase with different formulations. While the silane chemistry and its interactions with the glass surface and the polymer have been extensively studied, relatively little information is available about the influence of these sizing components on the formation of the interphase.

The interphase is the region where stress transfer occurs between the two composite constituents, but its material properties and effec-

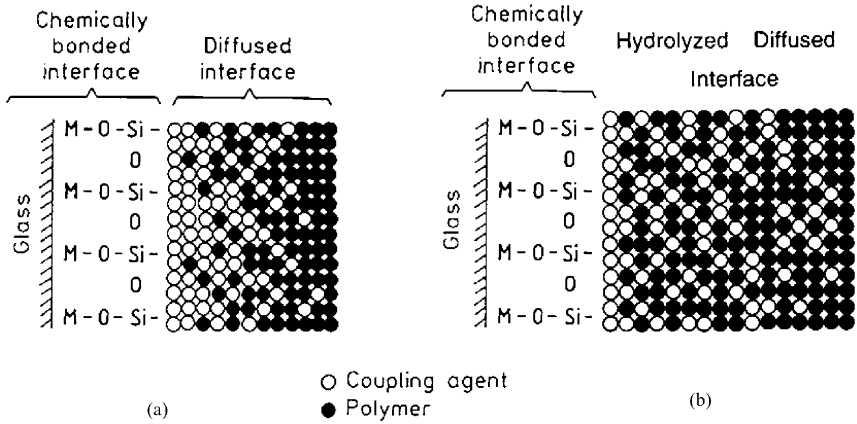

FIGURE 1 Schematic models for (a) conventional interdiffusion and IPN [18]; and (b) hydrolyzed diffused interface after ageing in water [45] in a silane treated glass fibre composite.

tive thickness are largely unknown. Investigation of the mechanical properties of the interphase presents a hard challenge to probing into materials in extremely low dimensions. Following the extensive studies in the past few years on this topic, this paper is aimed at providing an overview of the current progress and the state-of-the-art characterization techniques specifically developed for the measurement of thickness and properties of composite interphases. A number of techniques have been employed in the analysis of fibre surface layers, based on elemental chemistry, physics, and mechanical means. Apart from several spectroscopic analytical tools mentioned in the following section, special emphasis is placed on discussions of the novel techniques, such as the nanoindentation test, the nanoscratch test, and atomic force microscopy (AFM) in its various application modes along with the nanoindentation technique. However, no detailed discussions will be made on the interfacial adhesion strengths that are measured based on various micromechanics tests using microcomposites consisting of single fibres embedded within a matrix material, such as the fibre pullout test, the fibre pushout test, the fibre fragmentation test, and the microdroplet test. A comprehensive review of these testing methods is provided elsewhere [2].

CHARACTERISATION OF THE INTERPHASE USING SPECTROSCOPY

Several spectroscopic techniques have been successfully employed to quantify the rates of interdiffusion and chemical reactions between silane and polymer matrices. Solid-state nuclear magnetic resonance (NMR) spectroscopy of a phenolic polymer bonded to a silica surface was applied to measure the movement of adsorbed chain segments, revealing that the molecules of water can replace the polymer chain segments on the surface by diffusion to the interface [19, 20]. The randomly distributed oxide groups on the glass surface absorb water as a hydroxyl group. Hence, the untreated glass fibre composites were prone to degradation of mechanical properties under wet conditions.

The spectra obtained from FTIR spectroscopy [3–7] were useful to detect and analyze complex chemical reactions taking place between the glass surface and the silane agent applied in dilute aqueous solution. The molecular orientation of silanols at the surface enhanced the condensation rate, although some polymeric matrices could inhibit the reactions. The condensation reaction was reversible and controlled by pH of the solution and the presence of water, thus affecting the nucleation and growth rates of the polymerization process. Recent studies using evanescent wave FTIR spectroscopy were aimed at

monitoring chemical reactions between γ-aminopropyl-trimethoxy-silane (γ-APS)-treated glass fibre and an epoxy resin [21–23]. It was found [23] that there was a decrease of 13% in band absorbance when 5% silane was applied using a diluted solution, then 22% and 38% when silane agents were applied in 2% and 1% solutions, respectively. These results indicate that a significant fraction of the amine groups remain unreacted due to increased silane adsorption density and entrapment of silane molecules.

Ion scattering spectroscopy (ISS) and secondary ion mass spectroscopy (SIMS) were employed to characterize the morphology of a silane-treated glass-epoxy interphase [24]. The spectra revealed that the coating layer on the glass surface consisted of three layers with distinct properties: (1) a hard layer from the free surface to about 140 Å inside, (2) a soft oligomeric layer containing incompletely condensed siloxane between 140 Å and 240 Å away from the surface, and (3) a high molecular weight siloxane layer about 240 Å from the free surface and the glass surface. The siloxane layer was at least partially bonded covalently to the glass surface and differed in behaviour from the outermost two layers. These findings coincide with the early theory of three different chemical structural regions of the silane-treated interface, namely the physisorbed, chemisorbed, and chemically-reacted regions [12, 13].

More recently, X-ray photoelectron spectroscopy (XPS) [25–27] has been used as a means of characterizing glass fibre coatings by developing a protocol to plot ratios of appropriate atomic concentrations (C/Si and O/Si) at different depths of the surface layer. The plots of atomic concentrations were used to estimate the chemical composition and the surface coverage of the total glass surface layer [26], concluding that untreated glass fibre has a silica-rich surface as compared with the bulk of the fibre. The concentration of silicon in the surface layer further increased due to the presence of size containing silane coupling agents.

Although the above characterization tools were successfully employed to evaluate the physico-chemical properties of the glass surface such as chemical reactions, atomic structure, and molecular orientation, none of the above techniques were able to provide specific information about effective thickness of the interphase as an intermediate region between the reinforcement and the matrix material. An early study by infrared spectroscopy (IR) of epoxy matrix composites containing aramid and carbon fibres [28] may be the only one that offered an estimate an interphase thickness of 200–400 nm. The fibres were coated with a silane solution, which reacted with an anhydride-cured epoxy. The modification of crosslinking chemistry on

the fibre surface was detected, which was responsible for the formation of an interphase with properties different from those of the bulk matrix. A summary of this result along with interphase thickness and other properties reported in the subsequent studies on various combinations of fibre, matrix, and coupling agent are presented in Table 1.

STEREOSCOPIC DISPLACEMENT ANALYSIS

Apart from the physico-chemical analytical tools described above, the early attempt to measure the interphase thickness [29] was based on a high-resolution displacement measurement technique, along with the nanoindentation test discussed in the following section. In the so-called tensioned fibre method, which is similar to the fibre pullout test, the surface displacement in a disk of resin containing a single carbon fibre was measured while tension was applied to the fibre. A stereo imaging displacement analysis was used to obtain sub-micron spatial resolution and high displacement sensitivity. Figure 2 presents a typical topographic out-of-plane displacement map calculated from the micrographs taken in the unstressed state and after removal of the stress for the first loading/unloading cycle, while Figure 3 shows the corresponding out-of-plane displacements of the matrix relative to the fibre along the cross-section indicated in Figure 2. Quantitative interpretation of the elastic deformation map suggested that the fibre is surrounded by an interphase region of thickness of approximately 500 nm, which is soft and capable of very high deformation, with a depressed glass transition temperature. The observation of a soft interphase was considered to be consistent with the analysis of the fibre pushout test reported at almost the same time [30]. The presence of a stiff fibre mitigated the effect of a soft interphase, increasing the effective modulus of the interphase beyond that of the bulk matrix very near the fibre, as measured from the nanoindentation test [29].

NANOINDENTATION AND NANOSCRATCH TECHNIQUES

The use of nanoindentation and nanoscratch instruments to measure the mechanical properties of a fibre-matrix interphase is an inevitable choice due to the sub- or near-micron size of interphase to be probed. The nanoindentation test was originally designed to evaluate the material properties of thin films and coatings on a multilayer structure, which cannot usually be achieved using conventional microhardness testers, with reasonable resolution and accuracy [31]. The advantages of using the nanoindentation technique lies in the capability to produce very shallow indents, and there is much to be gained

TABLE I Summary of Previous Studies on Interphase Thickness and Properties

Fibre-matrix system	Testing technique	Interphase thickness	Modulus/hardness relative to matrix material	Reference
Kevlar®49 aramid-EPON828® epoxy Thornel T500® carbon-EPON828 epoxy	IR spectroscopy	200–400 nm	—	[28]
AS4 carbon-EPON828 epoxy	SEM stereo imaging displacement analysis	500 nm	Softer	[29]
Bare and γ-APS sized (in various film former) E-glass fibre-epoxy	AFM force modulation	$\sim$1–3 μm	—	[50]
HM carbon-polyphenylene sulfide	Force modulation AFM	20–80 nm	—	[51]
γ-APS silane treated E-glass-EPON828 epoxy	Interfacial force microscopy (IFM)	$\sim$8 μm	Varied	[49]
EPON1001F epoxy coated AS-4 carbon-EPON 828 epoxy	AFM indentation	Too small to detect	Similar to matrix	[57, 58]
Bare and γ-APS silane treated SiO_2-EPON828 epoxy	Phase imaging AFM and nanoindentation	2.4–2.9 μm independent of silane concentration	Softer	[54]
Commercial sized E-glass-polyester	Nanoindentation and nano-scratch	2–2.2 μm	Harder	[44]
Commercial sized E-glass-CL1880 phenolic		5.2–6.0 μm		
Commercial sized E-glass-CL1916 phenolic		3.4–3.7 μm		
Commercial sized E-glass-polyester (aged)	Nanoindentation and nanoscratch	4–5 μm	Harder	[45]

Commercial sized E-glass-CL1880 phenolic (aged)		5.5–10.0 μm		
Commercial sized E-glass-CL1916 phenolic (aged)		3.7–6.6 μm		
γ-MPS and γ-GPS silane treated glass-vinylester	Nanoindentation	~1 μm	Harder	[40]
	Nanoscratch	0.8–1.5 μm		
	DSC	1.3–1.7 μm		
γ-APS/PU sized E-glass-PPm	Phase imaging AFM and nanoindentation	100–300 nm depending on the type of sizing and matrix	Softer	[59, 60]
γ-APS/PP sized E-glass-PPm			Harder	
γ-APS/PU sized E-glass-epoxy			Property gradient	

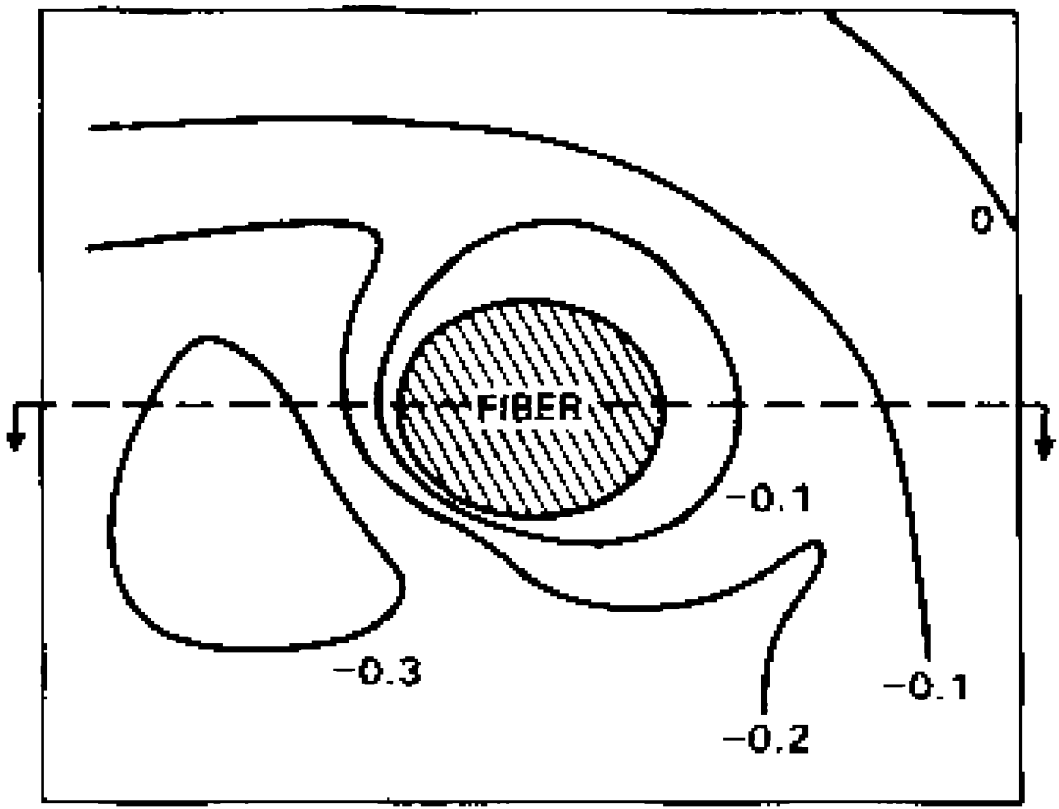

FIGURE 2 Topographic map of out-of-plane displacement after removal of the stress. After Williams *et al*. [29].

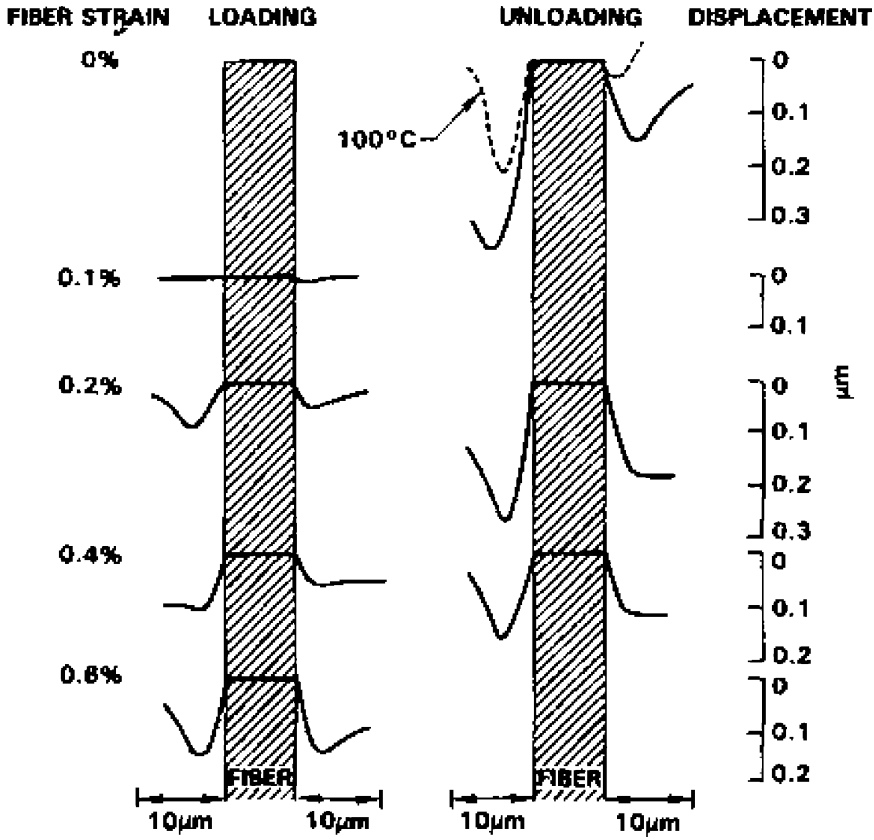

FIGURE 3 Out-of-plane displacement of the matrix relative to the fibre during the first loading and unloading cycle. After Williams *et al*. [29].

by applying the lowest possible indentation depths. The nanoinstruments can be classified into two different categories: one based on rigid foundation and positioning mechanisms without the capability of AFM (such as those from Nano-instruments and MTS). This type of nanoinstrument normally uses Berkovich diamond tips with a tip angle of 76.9° and a radius of about 50 nm, allowing higher load applications and tangential force measurements during the horizontal scratch. A typical Nano-Indentor II has an indentation vertical displacement resolution of 0.04 nm, an indentation placement resolution of 0.5 μm, and a load resolution of 50 nN. The other type, normally as part of an AFM (such as those from Digital Instruments and Hysitron Inc.), uses an indenter tip made from electrochemically sharpened tungsten or single-crystal silicon, with the nominal tip radius less

than 10 nm, attached to the end of a scanning cantilever to assure good imaging resolution and nanometer scale indents. With the rapid development of electronics and microscopy, it is now possible to achieve a displacement resolution of subnanometer scale and a load resolution of submicro Newton. A recently developed Hysitron Triboindenter has a transducer displacement resolution of 0.2 nm and a load resolution of less than 1 nN.

As for the conventional microhardness test, hardness is measured from the applied load divided by the projected contact area corresponding to the applied load. The depth sensor in the nanoindenter, normally too small to detected using an optical microscope, is calculated accurately during the loading cycle [32]. The hardness, H, and the reduced elastic modulus, E_r, are calculated based on the following equations, taking into account the effect of a non-rigid indenter column [31, 33]:

$$H = \frac{P}{A} = \frac{P}{24.5h_c^2}, \tag{1}$$

$$E_r = \frac{\sqrt{\pi}}{2\beta}\frac{S}{\sqrt{A}} = \left(\frac{(1-\upsilon_i^2)}{E_i} + \frac{(1-\upsilon_s^2)}{E_s}\right)^{-1}, \tag{2}$$

where P is the maximum load, A is the contact area, and h_c is the contact depth of indent. β is the geometric constant (=1.034 for a triangular indenter) and S is the unloading stiffness at maximum load. E and υ are the modulus and the Poisson ratio, and the subscripts i and s refer to the indenter and the specimen, respectively. The accuracy of indenter depth, load applied, and thus the measured properties are guaranteed only when the surface to be probed is metallographically smooth. This requires the specimen surface to be polished to make it almost perfectly flat and pit-free. Suspended fine ceramic particles, such as diamond or alumina, are normally used in a stepwise manner starting with coarse particles greater than 1 μm and finally finishing with ultrafine (0.05 μm) particles. This would produce a sample surface with a vertical range of 100–200 nm and an average roughness about 10–20 nm. There may be some adverse effects of lubricant or polishing medium adsorbed into the interphase polymer that have not been specifically studied previously.

Meanwhile, the nanoscratch technique has been extensively used to evaluate the adhesion, wear, and friction characteristics of thin films [34, 35], magnetic coatings and electronic materials [36–39]. The nanoscratch test involves moving the sample while in contact with the indenter tip, producing scratches in a straight line under a constant

normal force, N. The depth of the indenter is recorded, thus indicating the hardness of the surface being scratched. The tangential force option of the nanoindenter, equipped with a set of proximity probes and a special scratch-test collar, allows continuous measurements of the lateral deflection of the indenter shaft as well as the tangential force, F. The tangential force-displacement data can be obtained at an interval of a few nm, and the data are analyzed by plotting the scratch depth and/or the coefficient of friction ($\mu = \mathrm{F/N}$) *versus* the scratch length profiles.

As noted in the preceding section, the nanoindentation test was first successfully used to characterise a carbon fibre-epoxy interphase [29], revealing a higher modulus of the interphase than of the surrounding epoxy matrix, partly due to the influence of a nearby stiff carbon fibre. The authors [40] carried out the nanoindentation and nanoscratch tests on glass fibre-vinylester matrix composites with different silane coupling agents, such as γ-methacryloxypropyl-trimethoxysilane (γ-MPS) and γ-glycidoxypropyl-trimethoxysilane (γ-GPS), their concentrations being 0.01 wt%, 0.4 wt%, and 1.0 wt% (designated as M0.01, M0.4, and M1.0, respectively, for γ-MPS), which were applied onto the fibres in aqueous solutions of different silane concentrations. In the nanoscratch experiment, the effective interphase thickness was estimated,

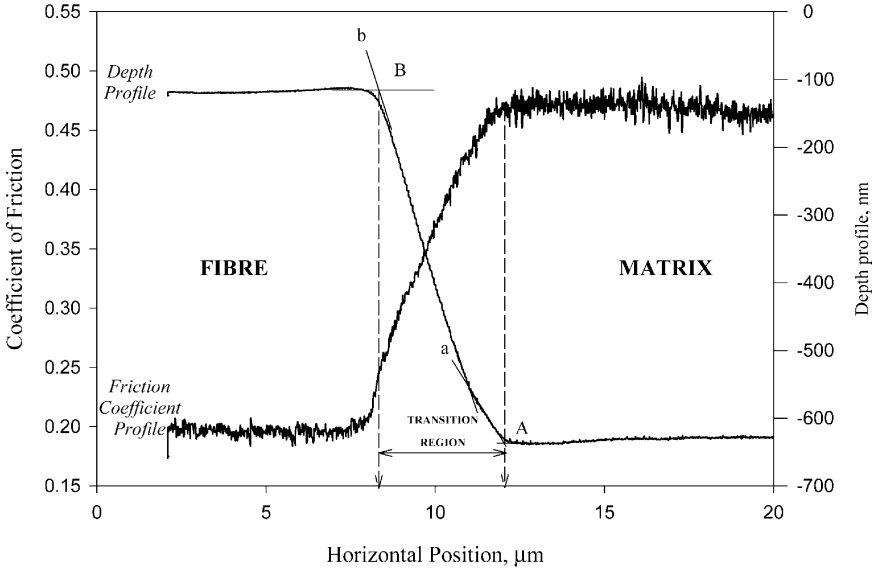

FIGURE 4 Coefficient of friction and scratch depth profiles obtained from the nanoscratch test at a constant normal load. After Kim *et al*. [40].

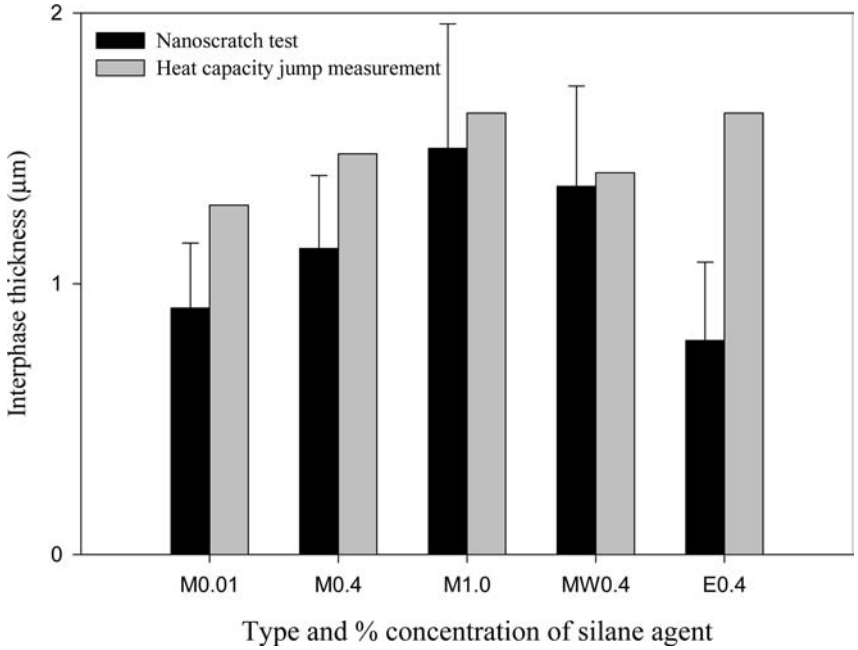

FIGURE 5 Effective interphase thickness values for composites with different silane agents measured based on nanoscratch test and the heat capacity jump measurement. After Kim *et al*. [40].

taking into account the scratch tip geometry and the interactions occurring between the scratch tip and the individual fibre-interphase-matrix components. Figure 4 presents the coefficient of friction and scratch depth profiles from which a transition region can be identified between fibre and matrix. The transition region comprised the genuine interphase, as well as the region created by the finite width of scratch tip, represented by the areas with two distinct slopes of scratch depth profile—a and b, respectively. The interphase modulus and effective thickness values thereby determined turned out to vary with silane type and concentration, indicating that the presence of a stiff fibre is not the only parameter influencing the test results, as the interphase hardness/modulus results showed higher values than that of the bulk vinylester matrix. The interphase thickness was approximately 1 μm from the nanoindentation test for all silane concentrations studied. It varied in the range of 0.8–1.5 μm from the nanoscratch test in which the effective interphase thickness increased consistently with increasing the silane concentration, as shown in Figure 5. The absolute magnitude and the general trend of interphase

thickness were consistent with the results obtained from heat capacity measurements based on differential scanning calorimetry (DSC). Figure 6 presents typical heat capacity curves at the respective glass transition temperatures, T_g, of unfilled and fibre-reinforced vinylester matrix. This observation confirms in part the validity of the nanoscratch test results on effective interphase thickness. The larger effective interphase thickness obtained for the fibres treated with higher concentration of the silane corresponds to a higher interfacial bond strength and higher composite tensile strength [41, 42].

A silane treated glass-vinylester interphase harder than the bulk matrix was consistent with earlier work on the properties of a simulated interphase [43]. The measured mechanical properties of the blends made from two typical epoxy matrices, three types of silane (such as APS, GPS, and MPS), and a commercial sizing at a concentration of about 14.5 phr suggested that the chemical/physical interaction of the silane and sizing with epoxy generates an interphase, whose properties are much different from the bulk matrix. The interphase had a lower T_g [29], a higher tensile strength and modulus

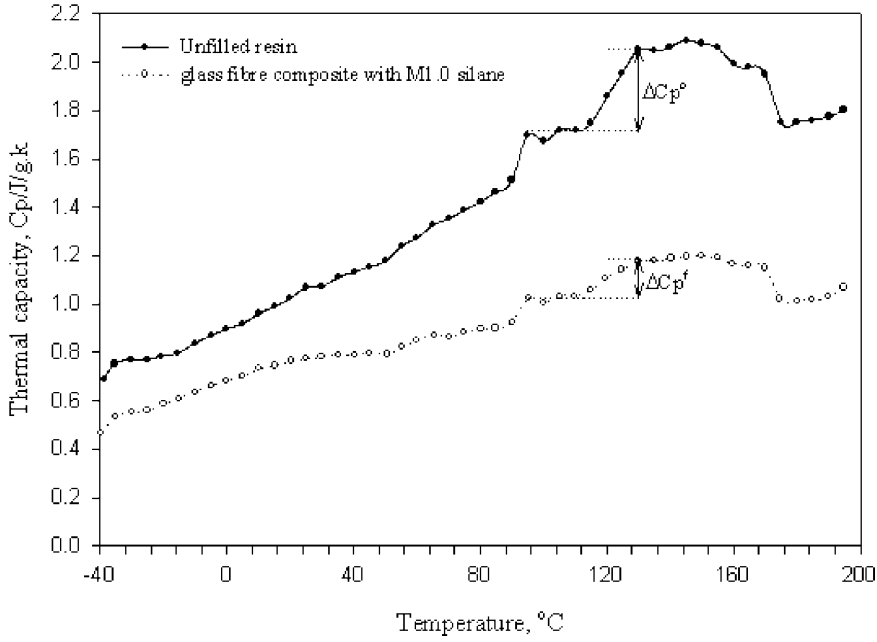

FIGURE 6 Typical specific heat capacity curves at glass transition region of unfilled and fibre reinforced vinylester matrix. After Kim *et al*. [40].

and lower fracture toughness than the bulk matrix material [43]. The silane and other ingredients contained in the size reduced the cross-linking density of the mixtures. The composites with such an interphase tended to have a higher interlaminar shear strength and a higher flexural strength than those without size applied to the fibre. This is attributed to the improved interfacial bond strength with the size, similar to the results shown above [41, 42].

The above promising results served as an impetus for further nanoindentation and nanoscratch experiments involving commercially sized E-glass fibres with polyester and phenolic systems after ageing in cold water for marine applications of these composites [44–46]. Indentations were made along a 14 μm-long path starting from the matrix and ending on the fibre to evaluate the effect of ageing in water on the degradation of the interphase properties. The distinct properties of the interphase were revealed by a sequence of 2–3 indents in the dry material and up to 15 indents in the aged specimens, as shown in Figure 7. The transition region observed between the fibre and matrix exhibited a similar characteristic in the dry condition for the polyester and phenolic systems. However, the hardness results varied for different matrix materials after ageing in water, with the interphase region in the phenolic system expanding several times, far beyond the area possibly affected by the fibre-stiffening effect. The corresponding increases in interphase thickness for the polyester system were relatively small. The mechanics analysis of the indentation test indicated that the size of matrix deformed by the indent was much smaller than the effective interphase thickness determined in the experiment. This further confirms that the interphase thickness does not merely represent the area influenced by the presence of a stiff fibre [44].

The nanoscratch test results also showed that the effective interphase thickness increased and the material properties degraded after water aging. Figure 8 presents typical depth profiles obtained from the nanoscratch test for both the polyester and phenolic systems, illustrating much different scratch behaviours between the specimens before and after ageing in water. The results obtained from the nanoscratch tests at two constant normal loads of 0.4 and 1.0 mN are compared with those from the nanoindentation tests in Table 2, which exhibited an essentially similar trend with respect to matrix material and ageing duration. It was postulated that the silane agent comprising three layers, namely the physisorbed, chemisorbed, and chemically reacted layers, reacted incompletely with the matrix polymer [12, 13]. In dry conditions, the results from both techniques showed a significantly hard portion of the interphase region, due mainly to the

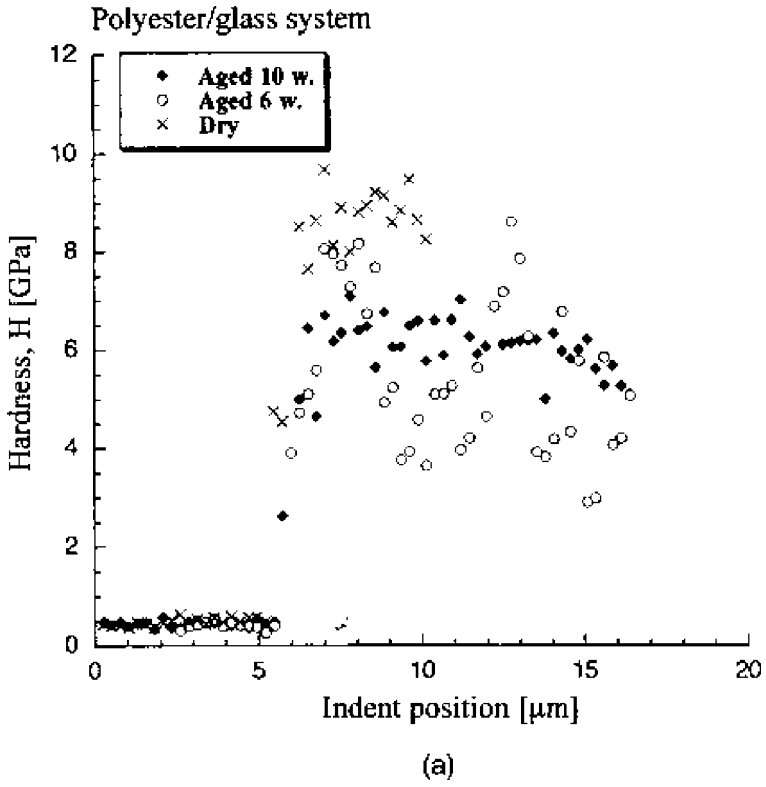

FIGURE 7 Hardness measurements of commercial sized (a) polyester-glass and (b) phenolic-glass interphase regions in dry conditions and after 3 and 10 weeks ageing in water. After Hodzic *et al*. [45]. (Continued).

innermost, chemically reacted layer. During aging in water, the non-reacted portion of the outermost, physisorbed layer dissolved deeply into the matrix assisted by the interdiffused water, *i.e.*, hydrolysis, at the interphase region, and the un-reacted silane chains were allowed to bond to the polymer molecules deeper into the matrix. Therefore, the initially hard part of the interphase formed an extended region of reacted silane molecules after aging in water. The resulting expanded interphase assisted by hydrolysis and interdiffusion is schematically presented in Figure 1b, as compared which the conventional IPN model shown in Figure 1a. The interphase degradation was confirmed by the single fibre microbond test, revealing losses in the glass fibre-matrix bond strength as well as in the bulk fracture properties [47, 48].

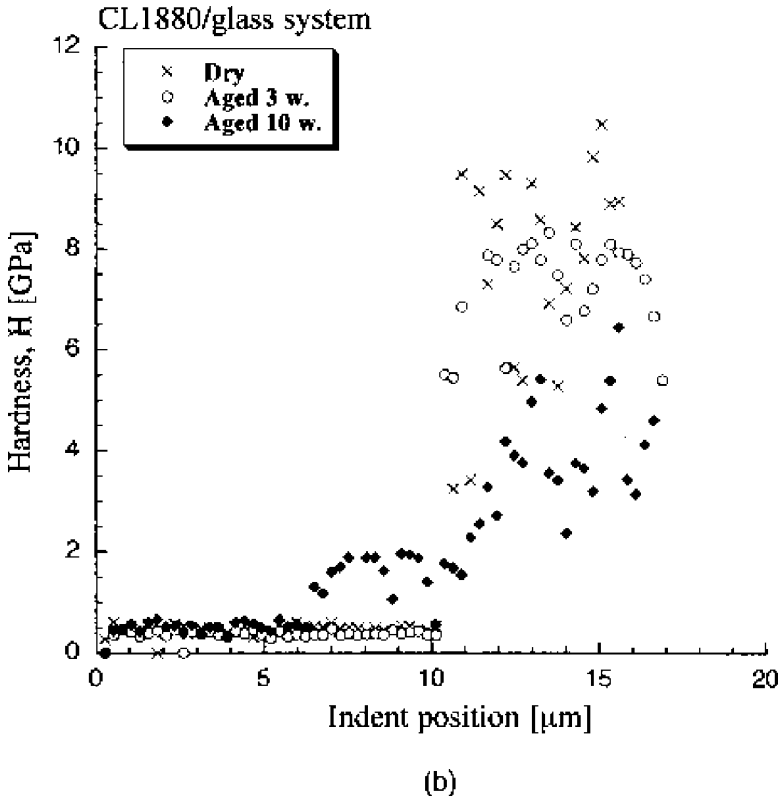

FIGURE 7 Continued.

ATOMIC FORCE MICROSCOPY: FORCE MODULATION, PHASE IMAGING, AND NANOINDENTATION

The initial attempt to measure the interphase thickness and properties using AFM or scanning force microscopy (SFM) was based on the contact mode and the force modulation mode [49–51]. In AFM, the indenter tip attached to the end of a silicon cantilever, having a high resonance frequency and high spring constant, scans across the polished specimen surface. The forces between the cantilever tip and the specimen introduce a bending of the cantilever, which is detected *via* a laser beam and a segmented photodiode. In the conventional contact mode, the repulsive forces are kept constant, and the output of feedback loop is used to construct the topographic image of the surface. Meanwhile, in the force or displacement modulation mode, the normal position of specimen or cantilever is modulated sinusoidally over a

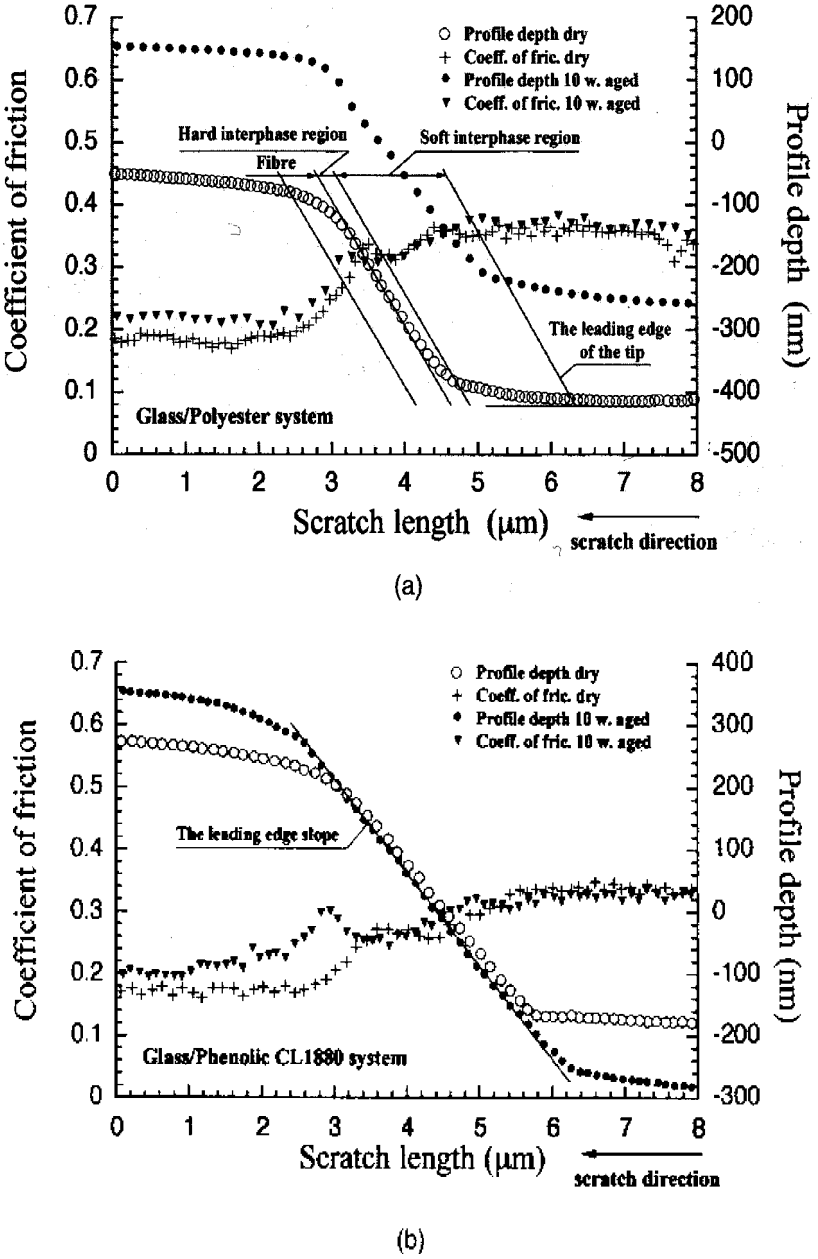

FIGURE 8 Typical coefficient of friction and scratch depth profiles obtained from the nanoscratch test at a constant normal load for commercial sized (a) polyester-glass and (b) phenolic CL1880-glass systems. After Hodzic *et al*. [45].

TABLE 2 Summary of Commercial Sized Glass-Polymer Interphase Thickness Measurements by Means of Nanoscratch and Nanoindentation Tests [45]

Glass-polymer system	Water ageing	Interphase thickness (μm)		
		Nano-scratch test		Nano-indentation test, depth = 30 nm
		F = 1 mN	F = 0.4 mN	
Polyester Synolite	dry	2.0	2.0	0.78
	3 weeks	2.31	2.06	1.3
	10 weeks	2.73	2.37	1.3
Phenolic CL1880	dry	3.35	1.91	0.78
	3 weeks	4.77	2.46	1.04
	10 weeks	5.07	2.6	5.72

small distance when the cantilever tip indents cyclically into the sample surface, allowing modulation of the load exerted by the tip or modulation of the bending of the cantilever, depending on the local specimen preparation [52]. This provides invaluable qualitative information about the local elasticity or compliance.

Mai and coworkers [50] did pioneering work on nanoscopic characterization of fibre surface and composite interphase based on the AFM. The AFM topographic images of glass fibres treated with γ-APS silane exhibited a rougher surface, with silane islets, than unsized glass fibres. The roughness of the glass fibres with γ-APS size in conjunction with a polyurethane film further increased due to the dispersed film former of the size. The force modulation AFM images along with the cross-sectional AFM topography allowed one to estimate the interphase thickness, based on the difference in darkness, which reflects the hardness of fibre, interphase, and matrix. The light gray region detected between the nearly white glass fibre and the darker bulk matrix in Figure 9 was identified as an interphase, whose thickness was approximated to be 1 μm for the unsized glass-epoxy system [50]. The interphase in the unsized glass-fibre composite was proven to be more brittle than the bulk matrix, while the interphase in the sized glass-fibre composite was more ductile, as confirmed in the fibre pullout test [53]. The 1 μm thick interphase in glass-epoxy systems appears to be much larger than the interphase thickness in the range of 20–80 nm for a carbon fibre-polyphenylene system that was determined using an essentially similar AFM technique [51]. In addition to the topographic analysis, the electrical and stiffness contrasts between the conductive fibre and the thermoplastic matrix were

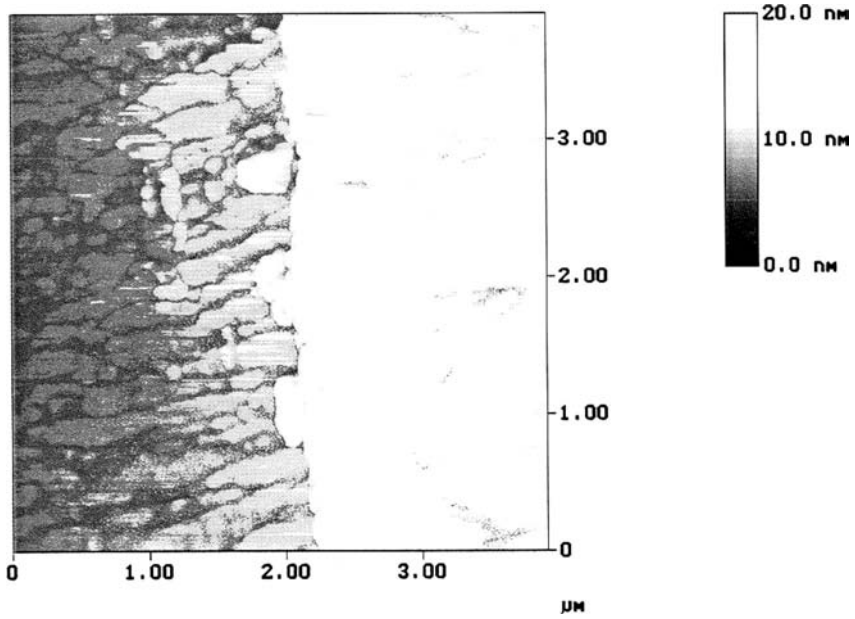

FIGURE 9 AFM force modulation mode image of an unsized glass-epoxy resin interphase. Reprinted from Mai, K., Mäder, E., and Mühle, M., Interphase characterisation in composites with new non-destructive methods, *Composites Part A* **29**, 1111–1119 (1998) [50], with permission from Elsevier Science.

utilized to determine the effective thickness of the interphase assuming a single-exponential decay of local stiffness along the distance from the fibre to the matrix. The interfacial force microscope (IFM), equipped with a self-balanced differential capacitance force sensor similar to the AFM's cantilever with a probe tip, was also successfully employed to obtain the indentation force-depth profiles for a γ-APS–treated glass fibre-EPON828 epoxy system [49]. The elastic modulus, calculated based on the Hertzian contact mechanics analysis, varied significantly within an 8 μm region between the fibre and bulk matrix, identifying an interphase that seems to be the thickest amongst those reported for similar glass-epoxy systems treated with silane agents (see Table 1).

As noted previously [29], the information about the properties of the interphase obtained from the force modulation mode of AFM may mislead, especially due to the presence of a fibre that is much stiffer than the surrounding interphase and polymeric matrix. The so-called "fibre stiffening" or "fibre bias" effect was specifically studied, showing that the modulus of the interphase next to the stiff fibre

approached that of the fibre near the fibre surface, while it decreased to that of the bulk polymer as the distance from the fibre increased [54, 55]. A similar result was reported previously [56–58] for carbon fibre composites and is confirmed by an axisymmetric finite element model. The area affected by the stiffening effect approximated 200–300 nm from the fibre surface for an unsized carbon-epoxy system [55, 56]. Once the fibre was removed by chemical etching, the gradient of modulus reversed itself. Figure 10 illustrates the AFM images of the composite interphase region before and after leaching fibers using hydrofluoric acid in this experiment. The indentation result suggests that nanoindentation based on the force modulation AFM is particularly inadequate for measuring the interphase properties. It was proposed that the "fibre bias" effect in nanoindentation could be reduced by reducing the indentation load and by cutting the sample at an angle [55]. It should be mentioned, however, that the etching agent used to remove the carbon fibre may have a damaging effect on the polymer surrounding the fibre, which was not specifically studied.

The phase imaging technique was thus developed [54, 59, 60], which involved a much lower interaction force between the probe and the sample than the force modulation AFM technique. Phase imaging

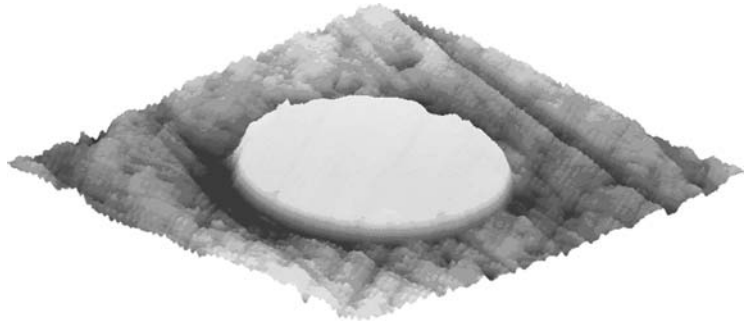

(a)

FIGURE 10 AFM images of γ-APS treated SiO_2-epoxy matrix composite (a) before and (b) after removal of fibre. Reprinted from Downing, T. D., Kumar, R., Cross, W. M., Kjerengtroen, L., and Kellar, J. J., Determination of interphase thickness and properties in polymer matrix composites using phase imaging atomic force microscopy and nanoindentation, *Journal of Adhesion Science & Technology* **14**, 1802–1812 (2000) [54], with permission from VSP International Science Publishers. (Continued).

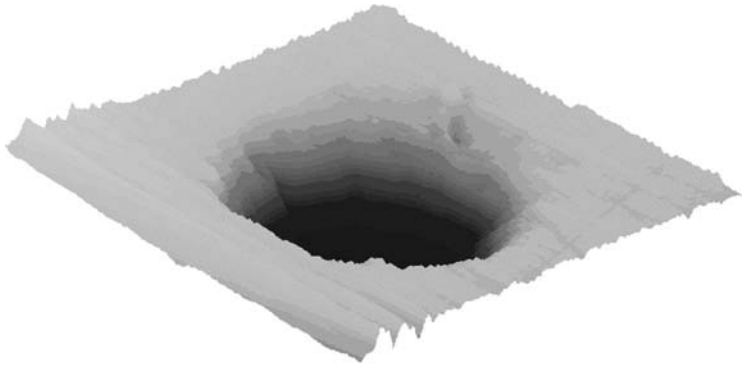

(b)

FIGURE 10 Continued.

based on tapping mode AFM measures the changes in the phase lag of the oscillation frequency, and the tip lightly impacts the sample surface during each oscillation cycle. Whilst the AFM topography cannot show apparent height differences, the cross-sectional analysis of the phase image can distinguish the individual fibre, matrix, and interphase regions, revealing differences in material properties. The phase image of γ-APS–treated SiO_2-epoxy interphase exhibited a bright area surrounding the stiff fibre, indicating a softer interphase region, similar to the result obtained from the samples with the fibre removed. γ-APS was applied in an aqueous solution without a film former. The measured interphase thickness in this case was 2.4–2.9 μm, irrespective of the γ-APS concentration, which ranged from 0.1% to 5% [54]. A representative phase image and the corresponding section analysis are presented in Figure 11, showing the interphase thickness and gradient. The interphase thickness was defined as the distance from the fibre where the property gradient decayed 90%, or to 10% of its initial value. The preferential adsorption of one component, usually the amine curing agent, with respect to the other components of the polymer was thought to be mainly responsible for the softer interphase and for essentially the same interphase thickness for all silane concentrations studied.

Based on the similar AFM phase imaging and nanoindentation techniques, Gao and Mäder [59, 60] made a comparative study of sized and unsized glass fibre surface topography and modulus, and mechanical property variations in the interphase formed with modified

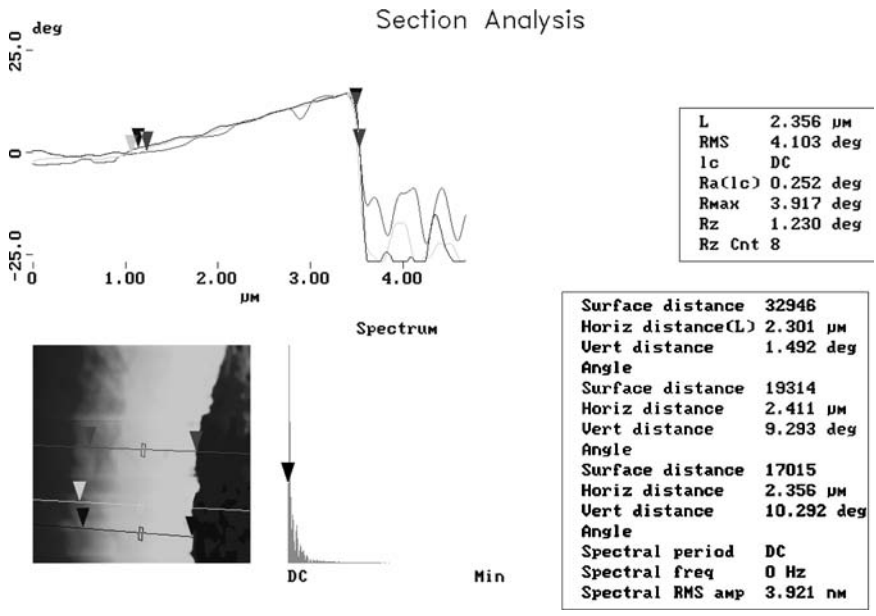

FIGURE 11 Section analysis of phase image showing interphase thickness in a γ-APS treated SiO_2-epoxy composite. Reprinted from Downing, T. D., Kumar, R., Cross, W. M., Kjerengtroen, L., and Kellar, J. J., Determination of interphase thickness and properties in polymer matrix composites using phase imaging atomic force microscopy and nanoindentation, *Journal of Adhesion Science & Technology* **14**, 1802–1812 (2000) [54], with permission from VSP International Science Publishers.

polypropylene (PP) and epoxy matrices. The sizes consisted of γ-APS as a coupling agent and polyurethane (PU) or PP dispersions as film formers. The phase image obtained from the γ-APS/PP sized glass-PPm system revealed an interesting size-induced transcrystallinity as shown in Figure 12. The PPm matrix near the fibre exhibited aggregation of radially oriented, sheaflike lamellae with a higher order of alignment and compact packing structure as a result of the spherulites emerging from the sizing surface and bulk matrix. The rough interphase had a thickness of approximately 100–200 nm (Figure 12a) and was quite uniform, with a few interphase layers reaching as far as 2 μm (Figure 12b) when excessive PP sizing was applied. In contrast, no such rough aggregates were observed in the γ-APS/PU sized glass-PPm system with quite uniform morphology, and there was rather a blurred boundary between the size and PPm matrix, attributed mainly to the partial miscibility, interdiffusion, and entanglement of polymer chains between the phases. The interphase showed a minimum phase

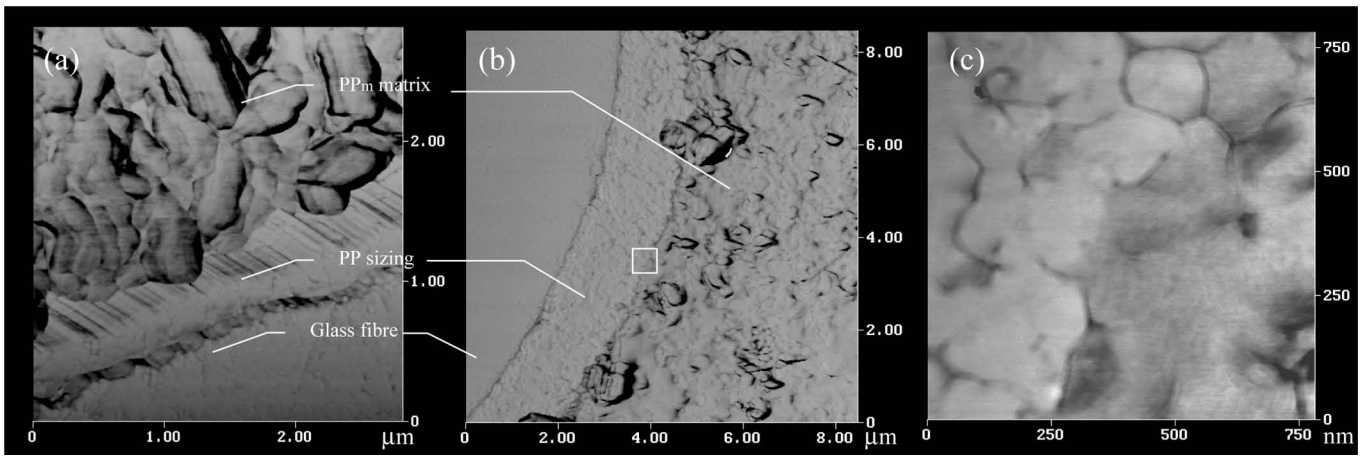

FIGURE 12 AFM phase images of interphase in γ-APS/PP-PPm composites. (c) illustrates a magnified view of the interphase/PPm region in (b). Reprinted from Gao, S. L. and Mäder, E., Characterisation of interphase nanoscale property variations in glass fibre reinforced polypropylene and epoxy resin composites, *Composites Part A* **33**, 559–576 (2002) [59], with permission from Elsevier Science.

angle compared with that of the matrix, indicating a low stiffness of interphase.

The AFM nanoindentation results confirmed the important differences in the characteristics of the two glass fibre-PPm interphases with different sizes. The interphase with γ-APS/PU sizing was much softer with some property gradient across the interphase, whereas the interphase with γ-APS/PP sizing was harder than the PPm matrix, with the hardness values being rather constant and independent of the distance from the fibre surface. The higher interphase modulus and interfacial bond strength for the γ-APS/PP sized glass-PPm system may have resulted in a higher composite tensile strength and Charpy impact toughness, as shown in Table 3, where the interphase and composite properties are compared for different sizing. It was suggested that the low-stiffness interphase in composites with γ-APS/PU size was able to separate the crystallization of modified PP from the fibre surface, as opposed to the case of γ-APS/PP sized fibre composites. The interphase in the γ-APS/PU sized glass fibre-epoxy system displayed a property gradient, as a reflection of the tendency of the amine curing agent to diffuse into the γ-APS/PU size, creating an amine-rich region near the fibre surface. Meanwhile, the unsized glass fibre-epoxy system did not show any trace of an interphase with a modulus different from the matrix, indicating that pure epoxy could not form an interphase at the unsized glass fibre surface.

Based on the above-mentioned results, three schematic models for interphase microstructure were proposed [59], as shown in Figure 13. The first and second models represent the γ-APS/PU and γ-APS/PP sizes with the PPm matrix, respectively, whose common structural features are summarized as follows: (1) the interphase prevents the PPm matrix from direct contact with the glass surface; (2) physical mechanisms, rather than chemical reactions, control the interphase modulus; (3) the adhesion between the fibre and interphase can be improved by removing the excessive physisorbed layers; and (4) the

TABLE 3 Comparison of Interphase Modulus, Interfacial Bond Strength, and Mechanical Properties of 13.4 vol% of Short Glass Fibre-modified Polypropylene Matrix Composites with Different Sizes [60]

Size	Interphase modulus [GPa]	Interfacial bond strength, τ_{app}[MPa]	Tensile strength [MPa]	Charpy unnotched impact toughness [kJ m^{-2}]
APS/PU-PPm	0.8 ± 0.5	10.9 ± 5.9	37.4	13.3
APS/PP-PPm	5.8 ± 0.7	21.7 ± 4.4	73.6	35.0

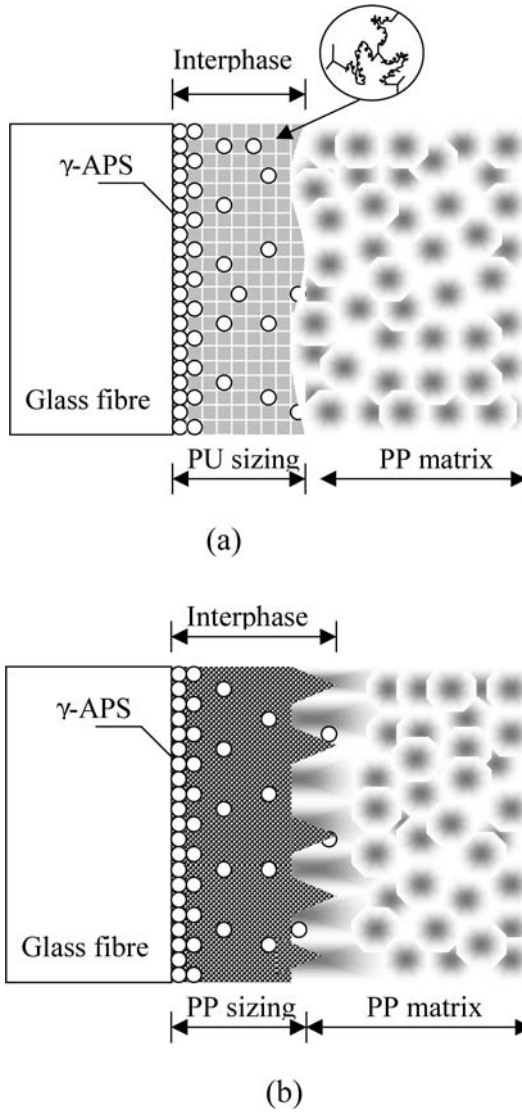

FIGURE 13 Schematic interphase models of two glass-PP systems with (a) γ-APS/PU and (b) γ-APS/ PP sizing, and (c) glass-epoxy system with γ-APS/PU sizing. Reprinted from Gao, S. L. and Mäder, E., Characterisation of interphase nanoscale property variations in glass fibre reinforced polypropylene and epoxy resin composites, *Composites Part A* **33**, 559–576 (2002) [59], with permission from Elsevier Science. (Continued).

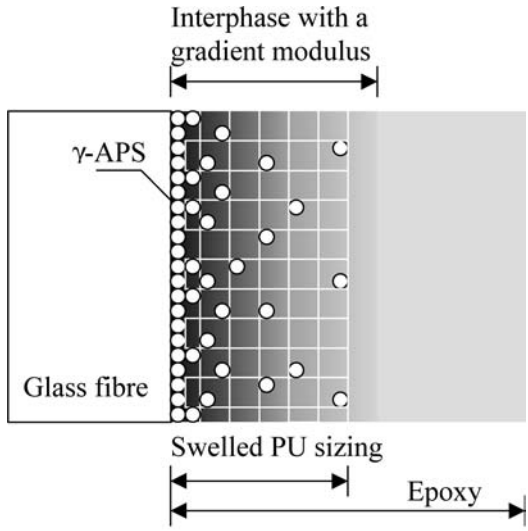

FIGURE 13 Continued.

γ-APS sizes have good wettability on the glass surface, giving rise to a strong interfacial bond. Therefore, chemical reactions are expected to occur between the sizes and functional groups from the PPm matrix. There are also differences between the two systems, namely the mechanical properties and morphology of their interphases, which in turn affect the mechanical properties and failure behaviour of composites with different sizings. Meanwhile, the third model represents the γ-APS/PU-epoxy interphase with a gradient modulus, which seems to be commonly present in suitably sized glass fibre-thermosetting systems. It was proposed that the composites with a property gradient interphase had better mechanical properties than those without such an interphase.

CONCLUDING REMARKS

An overview is presented in this paper regarding the current development of nanoscale characterization of the interphase in fibre-reinforced polymer matrix composites. Experience has shown that proper characterization of an interphase, whether it is for chemical, physical, or mechanical properties, is extremely difficult because the

interphase is on the microscopic, or often nanoscopic, scale and is buried within the composite body. Furthermore, there are seldom clear, distinct boundaries that would allow the interphase between the bulk fibre and matrix materials to be defined. This requires the characterization and measurement techniques to be of ultrahigh magnification and resolution for accurate and reproducible solutions. Amongst the various tools, nanoindentation, nanoscratch tests, and AFM along with the nanoindentation technique are identified as the useful methods that have been successfully applied to characterise the effective thickness and properties of interphase with acceptable accuracy and reproducibility. In particular, the phase imaging AFM technique is demonstrated to provide unique information on phase contrasts between the fibre, matrix, and interphase regions, from which the boundaries between these constituents can be identified.

Major limitations of the nanoindentation and nanoscratch experiments lie in the limited spatial sensitivity of the instrument to produce indents on the sample surface and to measure the relevant properties. This is especially true for testing with an indenter tip of finite radius, and its physical contact with a rough sample surface, to produce permanent indents whose dimensions are the same order of magnitude as the indenter tip radius or sample surface roughness. While the specifications of these instruments claim admirable capabilities, in reality these sensitivities can hardly be achieved due to the requirement of minimum space that has to be allowed between adjacent indents to avoid overlapping.

Whether the interphase material surrounding the reinforcements is softer or harder than the bulk matrix material has been of much interest to design engineers and materials scientists, because these properties influence significantly the overall mechanical performance of bulk composites. Carefully-executed experiments involving nanoindentation after removal of fibre proved that there is a significant "fibre stiffening" or "fibre bias" effect, which may erroneously result in a hard interphase in the vicinity of a fibre for an apparently soft interphase. This is particularly true for the indents produced with high indentation loads and penetration depths.

Taking into account the above "fibre stiffening" effect, opinions are still divided over the modulus/hardness of an interphase relative to the bulk matrix. Different models reported in the literature could be explained by different interdiffusion behaviour, chemical reactions, and molecular conformation taking place at the interphase region in different composite systems. From the results presented in this report, it can be concluded that the formation of both softer and harder interphases is possible, depending on the combination of

reinforcement, matrix, and coupling agent applied. Several studies proved that the interphase modulus/hardness could be tailored for particular end applications by proper selection of coupling agent not only for thermoset but also for thermoplastic matrix composites.

The effective thickness of the interphase varied significantly, depending mainly on the presence of sizing at the interphase region and the type of matrix material. Silane-treated glass fibres embedded in a thermoset matrix, such as epoxy, vinylester, and phenolic, created an interphase of 1 μm or thicker, and this size expanded up to several times upon ageing in water as a result of hydrolysis-assisted interdiffusion of silane agent. For composites made from unsized carbon fibre or PP matrix, the interphase thickness was almost an order of magnitude smaller; say, less than 300 nm, due to the lack of interdiffusion. While the presence of size or silane coupling agent on the fibre surface played an important role in creating an interphase of finite thickness, there are other environmental factors, as well as thermal, chemical, physical, and mechanical phenomena taking place during the various processing conditions, that are equally important depending on the type of fibre and matrix involved. These phenomena include the adsorption of gaseous species onto the fibre and dissolution of these species into the matrix during curing, the cross-linking process of matrix resin, the chemical reactions between various functional groups in the fibre surface and matrix material, and the volumetric changes and the generation of residual stresses from thermal and chemical sources. The interphase thickness is not solely determined by the silane thickness diffused into the matrix. It is not the silane concentration itself but the ensuing phenomena taking place in the presence of silane and other sizing ingredients that are more responsible.

The subject area discussed in this paper is still young within the broad composite engineering discipline, for which the test methods and measurement techniques have yet to be fully and extensively developed. While the data compiled above are far from complete and are confined to a few combinations of composite constituents, continued efforts are being made in several research groups around the world to improve further the accuracy and reproducibility of experiments based on improved instrumentation and novel techniques.

REFERENCES

[1] Drzal, L. T., Rich, M. J. and Lloyd, P. F., *J. Adhesion* **16**, 1–30 (1983).
[2] Kim, J. K. and Mai, Y. W., In *Engineered Interfaces in Fiber Reinforced Composites* (Elsevier Science, New York, 1998), chap. 7.
[3] Ishida, H. and Koenig, J. L., *J. Colloid Interface Sci.*, **64**, 555–565 (1978).

[4] Ishida, H. and Koenig, J. L., *J. Polym. Sci. Part B, Polymer Phys. Ed.* **17**, 615–626 (1979).
[5] Ishida, H. and Koenig, J. L., *J. Polym. Sci. Part B, Polymer Phys. Ed*. **18**, 233–237 (1980).
[6] Chiang, C. H., Ishida, H. and Koenig, J. L., *J. Colloid Interface Sci.* **74**, 396–404 (1980).
[7] Chiang, C. H., Liu, N. I. and Koenig, J. L., *J. Colloid Interface Sci.* **97**, 308–313 (1984).
[8] Kim, J. K. and Mai, Y. W., *Compos. Sci. Technol.* **41**, 333–378 (1991).
[9] Drzal, L. T. and Madhukar, M., *J. Mater. Sci*. **28**, 569–610 (1993).
[10] Loewenstein, K. L., Fibre sizes for continuous glass fibres. In *The Manufacturing Technology of Continuous Glass Fibres* (Elsevier, Amsterdam, 1983), 3rd ed., chap. 6, pp. 243–296.
[11] Gorowara, R. L., Kosik, W. E., McKnight, S. H. and McCullough, R. L., *Composites Part A* **A32**, 323–329 (2001).
[12] Schrader, M. E., *J. Adhesion* **2**, 202–212 (1970).
[13] Schrader, M. E. and Block, A., *J. Polym. Sci., Part C, Polym. Symposia* **34**, 281–291 (1971).
[14] Plueddemann, E. P., Clark, H. A., Nelson, L. E. and Hoffmann, K. R., *Modern Plastics* **39**, 135 (1962).
[15] Plueddemann, E. P., *Silane Coupling Agents* (Plenum Press, New York, 1982).
[16] Schrader, M. E., Lerner, I. and D'oria, F. J., *Modern Plastics* **45**, 195 (1967).
[17] Koenig, J. L. and Emadipour, H., *Polym. Composites* **6**, 142–150 (1985).
[18] Plueddemann, E. P., In *Proc. ICCI-II, Interfaces in Polymer, Ceramic and Metal Matrix Composites*. H. Ishida, Ed. (Elsevier, New York, 1988), pp. 17–33.
[19] Droste, D. H., DiBenedetto, A. T. and Stejskal, E. O., *J. Polymer Sci. Ser A-2* **9**, 187–195 (1971).
[20] Alber, K., Pfleiderer, B., Bayer, E. and Schnabel, R., *J. Colloid Interface Sci.* **142**, 35–40 (1991).
[21] Nishio, E., Ikuta, N., Okabayashi, H. and Hannah, R., *Appl. Spec.* **44**, 614 (1990).
[22] Leyden, D. E. and Atwater, J. B., In *Silanes and Other Coupling Agents*, Mittal, K. L., Ed. (VSP, Utrecht, The Netherlands, 1992), pp. 143–157.
[23] Connel, M. E., Cross, W. M., Snyder, T. G., Winter, R. M. and Kellar, J. J., *Composites Part A* **29**, 495–502 (1998).
[24] DiBenedetto, A. T. and Scola, D. A., *J. Colloid Interface Sci.* **64**, 480–491 (1978).
[25] Briggs, D. In *Practical Surface Analysis: Auger and X-ray Photoelectron*. Briggs, D. and Seah, M. P., Eds. (Wiley, Chichester, 1995), pp. 437–484.
[26] Thomason, J. L. and Dwight, D. W., *Composites Part A* **30**, 1401–1413 (1999).
[27] Thomason, J. L. and Adzima, L. J., *Composites Part A* **32**, 313–321 (2001).
[28] Garton, A. and Daly, J. H., *Polym. Composites* **6**, 195–200 (1985).
[29] Williams, J. G., Donnellan, M. E., James, M. R. and Morris, W. L., *Mat. Sci. Eng.* **A126**, 305–312 (1990).
[30] Tsai, H. C., Arocho, A. M. and Gause, L. W., *Mat. Sci. Eng.* **A126**, 295–304 (1990).
[31] Oliver, W. C., Hutchings, R. and Pethica, J. B., In *ASTM STP 889*, Blau, P. J. and Lawn, B. R. Eds. (American Society for Testing and Materials, Philadelphia, 1986), pp. 90–108.
[32] Bhushan, B., *Handbook of Micro/Nanotribology* (CRC Press, Inc., Boca Raton, Florida, USA, 1995), chap. 9.
[33] McAdams, S. D., Tsui, T. Y., Oliver, W. C. and Pharr, G. M., *Mat. Res. Soc. Symp. Proc.*, Materials Research Society, Pittsburgh, Pennsylvania, USA, (1995), vol. 356, pp. 809–814.

[34] Baljon, A. R. C. and Robbins, M. O., Adhesion and Friction of Thin Films. *MRS Bulletin*, **22**, 22–26 (1997).
[35] Steinmann, P. A., Tardy, Y. and Hintermann, H. E., *Thin Solid Films* **154**, 333–349 (1987).
[36] Wang, H. F., Nelson, J. C., Gerberich, W. W. and Deve, H. E., *Acta Metall. Mater.* **42**, 695–700 (1993).
[37] Bhushan, B. and Koinkar, V. N., *Appl. Phys. Lett*. **64**, 1653–1655 (1994).
[38] Kim, D. H., Kim, J. K. and Hwang, P., *Thin Solid Films* **360**, 187–194 (2000).
[39] Kim, W. S., Kim, J. K. and Hwang, P., *J. Electronic Mater.* **30**, 503–512 (2001).
[40] Kim, J. K., Sham, M. L. and Wu, J., *Composites Part A* **32**, 607–618 (2001).
[41] Sham, M. L., Kim, J. K. and Wu, J. S., *Polym. Compos*. **5**, 165–175 (1997).
[42] Kim, J. K., Sham, M. L., Hamada, H., Hirai, Y., Fujihara, K., Saidpour, H., Sezen, M., Dong, Y. J., Yang, H. S., Bai, Y. L., Mao, T. X., Bathias, C., Hoa, S. V., Boutella, A., Ngo, A. D., Krawczak, P., Bequignat, R., Pabiot, J., Pinter, S., Banhegyi, G., Drzal, L. T., Ho, H., Yue, C. Y., Padmanabhan, K., Suzuki, Y., Tanimoto, T., Schulte, K., Karger-Kocsis, J. K., Cantwell, W. J., Zulkitli, R., Ye, L., Lesko, L. J. and Garcia, K., *Composite Interfaces* **7**, 227–242 (2000).
[43] Al-Moussawi, H., Drown, E. K. and Drzal, L. T., *Polym. Compos*. **14**, 195–200 (1993).
[44] Hodzic, A., Stachurski, Z. H. and Kim, J. K., *Polymer* **41**, 6895–6905 (2000).
[45] Hodzic, A., Kim, J. K. and Stachurski, Z. H., *Polymer* **42**, 5701–5710 (2001).
[46] Hodzic, A., Kim, J. K. and Stachurski, Z. H., *J. Mater. Sci. Lett*. **19**, 1665–1667 (2000).
[47] Hodzic, A., Kim, J. K., Lowe, A. E. and Stachurski, Z. H., *Compos. Sci. Technol*. In press (2003).
[48] Hodzic, A., Kim, J. K. and Stachurski, Z. H., *Polym. Compos.* **9**, 499–508 (2001).
[49] Winter, R. M. and Houston, J. E., In *Proceedings of the SEM Spring Conference on Experimental and Applied Mechanics*, Society for Experimental Mechanics (SEM) Bethel, CT, USA, (1998), pp. 355–358.
[50] Mai, K., Mäder, E. and Mühle, M., *Composites Part A* **29**, 1111–1119 (1998).
[51] Munz, M., Sturm, H., Schulz, E. and Hinrichsen, G., *Composites Part A* **29**, 1251–1259 (1998).
[52] Maivald, P., Butt, H. J., Gould, S. A. C., Prater, C. B., Drake, B., Gurley, J. A., Elings, V. B. and Hansma, P. K., *Nanotechnology* **2**, 103–106 (1991).
[53] Mäder, E., Mai, K. and Pisanova, E., *Composite Interfaces* **7**, 133–147 (2000).
[54] Downing, T. D., Kumar, R., Cross, W. M., Kjerengtroen, L. and Kellar, J. J., *J. Adhes. Sci. Technol*. **14**, 1802–1812 (2000).
[55] Kumar, R., Cross, W. M., Kjerentroen, L. and Kellar, J. J., *Composite Interface*, in press (2003).
[56] Vanlandingham, M. R., McKnight, S. H., Palmese, G. R., Elings, J. R., Huang, X., Bogetti, T. A., Eduljee, R. F. and Gillespie, J. W., Jr., *J. Adhesion* **64**, 31–59 (1997).
[57] Vanlandingham, M. R., Dagastine, R. R., Eduljee, R. F., McCullough, R. L. and Gillespie, J. W., Jr., *Composites Part A* **30**, 75–83 (1999).
[58] Bogetti, T. A., Wang, T., Vanlandingham, M. R. and Gillespie, J. W., Jr., *Composites Part A* **30**, 85–94 (1999).
[59] Gao, S. and Mäder, E., *Composites Part A* **33**, 559–576 (2002).
[60] Gao, S. L. and Mäder, E., *Proc. ICCM-13*, Beijing, China, June 2001. Paper ID 1605.